

Study of Pipeline Steels with Acicular Ferrite Microstructure and Ferrite-bainite Dual-phase Microstructure

Xiurong Zuo^{a}, Zhengyue Zhou^a*

^aSchool of Physics and Engineering, Zhengzhou University, Zhengzhou, 450052, PR, China

Received: December 11, 2013; Revised: January 11, 2015

Three kinds of X70 steels with the same chemical composition and different microstructures fabricated by varying processes were compared in aspect of the microstructures and mechanical properties using SEM, TEM and tensile testing machine. The experimental results showed that the steel 1 with acicular ferritic microstructure fabricated by thermal-mechanical processing with online accelerated cooling (TMCP) exhibited an excellent combination of strength and toughness, but provided high yield ratio of 0.85, low uniform elongation of 8.3% as well as low strain hardening exponent of 0.09, indicating poor deformability. In contrast to above steel 1, the steel 2 and steel 3 having ferrite-bainite dual-phase microstructure respectively fabricated by TMCP and intercritical annealing exhibited the improved deformability in terms of the low yield ratio of 0.69 and 0.68, high uniform elongation of 12.8% and 11.8%, and strain hardening exponent of 0.157 and 0.155. It is argued that the optimum properties combination of strength, toughness and deformability can best be achieved by obtaining a ferrite-bainite dual-phase microstructure. This kind of ferrite-bainite dual-phase pipeline steel is appropriate to transmitting oil and natural gas in seismic zone and permafrost.

Keywords: *pipeline steel, dual-phase microstructure, ferrite, bainite, deformability*

1. Introduction

Pipeline steels are usually used to transport crude oil or natural gas over a long distance. In this condition, high strength and toughness are usually required. For X70 pipeline steel, an acicular ferritic microstructure is an optimal microstructure because of its excellent combination of strength and toughness. The microstructure of acicular ferrite consists of massive ferrite, granular ferrite, and bainitic ferrite with high density of dislocations and second phases islands in the matrix¹. A low-carbon Mn-Mo-Nb-Ti microalloyed pipeline steel can promote the acicular ferrite transformation². However, pipeline steel with this kind of microstructure possesses high yield ratio³, indicating poor deformability.

Dual-phase steel (DP) with ferrite plus martensite/bainite phases can be fabricated by heat treating in the intercritical region ($\alpha+\gamma$) or by TMCP processes, which has a low yield ratio and rapid strain hardening rate at the onset of plastic deformation, thereby, excellent deformability can be attained^{4,6}. Generally, the microstructure and mechanical properties of DP steel depend on their chemical composition and process parameters⁷⁻⁹. DP steel has been widely used in automotive industry at present.

At present, long-distance oil/gas transmission with pipeline steel is the most economical and safe method, but the pipeline traversing seismic zone and permafrost is prone to deformation¹⁰. The combination of high strength, high toughness and deformability is important requirements for the pipeline steel in such a severe environment. So DP steel with an excellent combination of deformability and

strength is a judicious selection for pipeline steel with high deformability.

Acicular ferrite X70 pipeline steel and dual-phase X70 pipeline steel can be produced by two different TMCP process through the controlling of rolling parameters and cooling conditions. At the same time, dual-phase X70 steel can also be fabricated by intercritical annealing with acicular ferrite X70 pipeline steel. These three kinds of X70 steels with the same chemical composition fabricated by different processes were compared in aspect of the microstructures and mechanical properties in the present work. The results will be beneficial to the practical application of ferrite-bainite dual-phase pipeline steels with high deformability.

2. Experimental Procedures

The explored material was X70 pipeline steel with a chemical composition (wt.%): 0.07C, 1.54Mn, 0.011P, 0.0009S, 0.14Si, 0.17Ni, 0.020Al, 0.06Nb, 0.17Mo, 0.013Ti and Fe balance. Two different hot rolling schedules were respectively conducted through controlling the rolling process and the cooling rate on a Steckel mill in order to obtain an acicular ferrite microstructure steel named steel 1 and a ferrite-bainite dual-phase microstructure steel named steel 2. And then, the steel 1 was heat treated in the intercritical region ($\alpha+\gamma$) obtaining a ferrite-bainite dual-phase microstructure steel named steel 3.

Microstructure examination of the steels was performed using JSM6700F scanning electron microscope. Samples were prepared following standard metallographic

*e-mail: zuoxiurong@126.com

procedures. The polished specimens were etched with 4 pct nital solution for microstructure observation. Substructures were examined by transmission electron microscopy (TEM, JEM 2100 with 200 kV). For TEM observation, thin foils were prepared by a twin-jet polishing technique. The tensile samples with a gauge length of 50.8 mm and a gauge diameter of 38.1 mm were prepared in the longitudinal direction of the rolled plates. The mechanical properties were tested at room temperature and the tensile speed was 1.0 mm/min. In order to evaluate the low-temperature toughness, standard charpy test specimens (10×10×55 mm) were prepared and tested at 253 K (−20 °C) on an impact testing machine in the transversal direction. Drop-weight tear test (DWTT) was tested at 258 K (−15 °C) in the transversal direction.

3. Results and Discussion

3.1. Microstructure

Figure 1 shows the microstructures of steels by different processes. The steel 1 in Figure 1a,b exhibited the acicular ferrite (AF) microstructure mainly consisting of massive ferrite, granular ferrite and bainitic ferrite with widely dispersed martensite/austenite (M/A) islands and little bainite in the matrix. The prior austenite grain boundary was eliminated, because the nucleation of AF was mainly on dislocations, inclusions such as complex oxides or sulphides and the growing austenite/ferrite interface¹¹.

By adjusting the parameters of TMCP, a dual-phase microstructure of polygonal ferrite (PF) plus bainite colonies at ferrite grain boundaries can be obtained in steel 2 (Figure 1c,d). During hot rolling process on a steckel

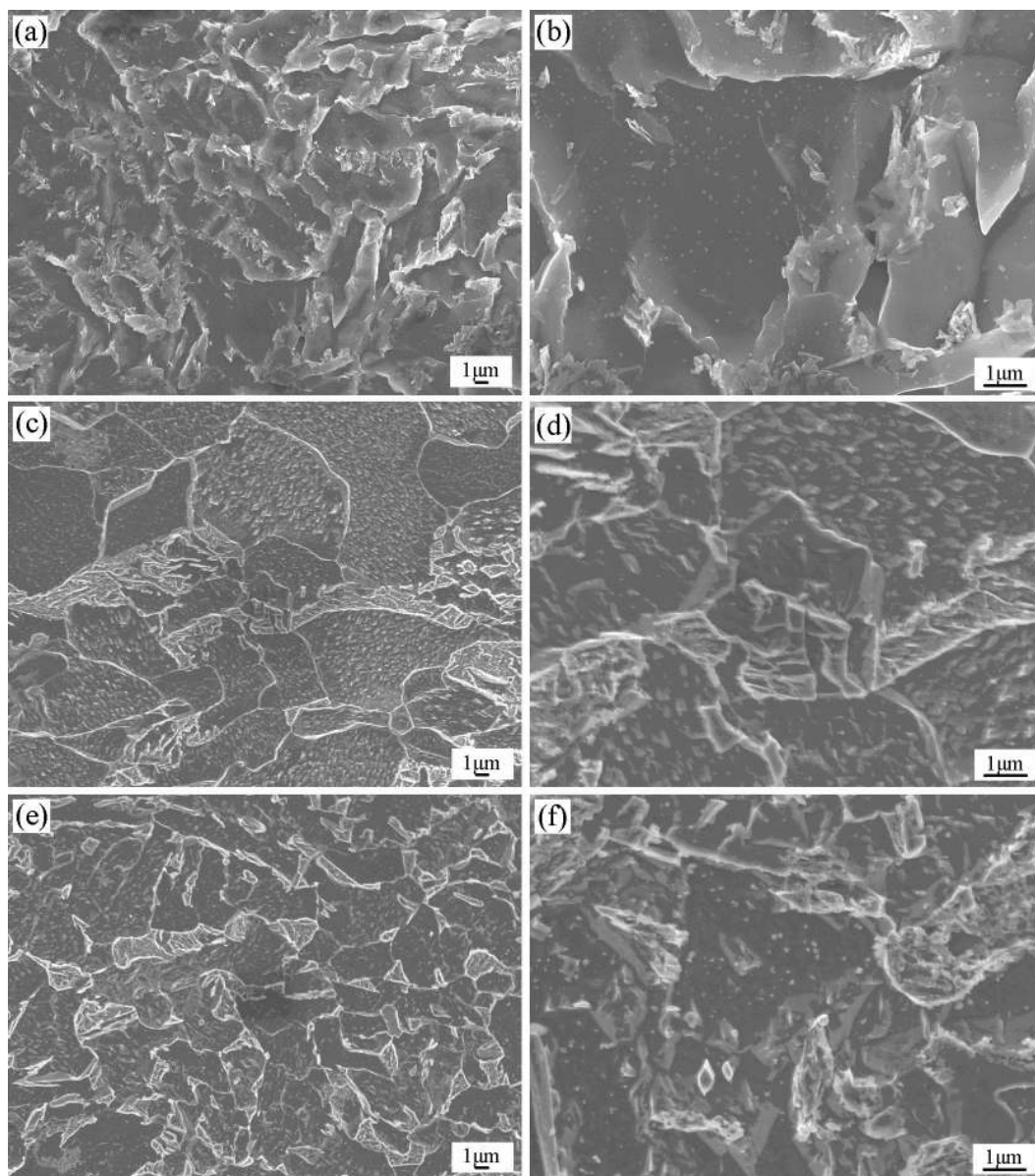


Figure 1. SEM images of experimental steels (a)(b) Steel 1; (c)(d) Steel 2; (e)(f) Steel 3.

mill, the steel was first preheated in a soaking furnace, and then cooled to the rolling temperature above non-recrystallization to roll. And then, the steel was cooled below non-recrystallization temperature and subsequently rolled in non-recrystallization region. After that, the steel was air-cooled for some time followed by water-jet cooling. Deformation in non-recrystallization region made the austenite grains elongate, leading to a high surface to volume ratio. The ferrite phase mainly nucleated at the former austenite grain boundaries, triple junctions and shear bands of the deformed austenite¹², so higher nucleation sites existed for PF during air-cooling process. With the formation of PF, austenite was carbon-enriched because of the partitioning of carbon to the austenite during the transformation to ferrite. With accelerating cooling after air cooling, most of the carbon-enriched austenite was transformed to bainite in the ferritic matrix.

By intercritical annealing with steel 1, the steel 3 with blocky bainite phases uniformly distributing in the ferrite matrix can be obtained (Figure 1e,f). This is because that, with the heating temperature in two-phase region, part of the acicular ferrite began to transform to austenite, which nucleated mainly in the original acicular ferrite grain boundary, M/A islands and little bainite. The fine acicular ferrite grain distributing in a chaotic manner with random orientations made austenite uniformly distribute in the ferrite matrix, leading to the uniform distribution of bainite compared to the steel 2. The soaking temperature and soaking time in two-phase region determined the volume fraction of austenite. During the cooling process, the austenite size firstly decreased by epitaxial ferrite growth on retained ferrite, at the same time, the remaining austenite enriched in carbon, which transformed to bainite with further cooling.

It should be noticed from the microstructure characteristics of acicular ferrite revealed in Figure 1 that precipitates containing Nb and Ti were remarkable in AF in steel 1 in comparison with those in PF in steel 2 and steel 3. The Precipitates are mainly (Ti,Nb)N, (Ti,Nb)C and (Ti,Nb)C₂N¹³. During preheating in soaking furnace before rolling, the microalloying elements were dissolved. Deformation of austenite during rolling introduced dislocations and vacancies which assisted the diffusion of the microalloying elements. For steel 1, after the finish rolling in the non-

recrystallization region of austenite, rapid cooling was immediately imposed by water jet. Supersaturation of these solute elements increased with temperature decreasing and precipitation occurred at the prior austenite grain boundaries or lattice defects during rapid cooling process. For steel 2, after the finish rolling in the non-recrystallization region, air cooling was imposed, afterward the steel 2 was rapidly cooled. Precipitation occurred during air-cooling process at higher temperature and subsequent rapid water-cooling process, so the precipitates were larger and more inhomogeneous in the ferritic matrix in steel 2 than those in steel 1.

The TEM features of the experimental steels are presented in Figure 2. It can be observed that the steel 1 produced by TMCP showed an acicular ferrite microstructure by non-equiaxial ferrite and an assemblage of interwoven nonparallel ferrite laths with dense dislocations and M/A islands which were formed mostly at the grain boundaries of the acicular ferrite (Figure 2a). In steel 2 and steel 3, the round thick M/A islands can be found distributing at the triangular grain boundary of PF which possessed far lower dislocation density than AF in steel 1. Because of fine acicular ferrite, the shape of M/A island in steel 1 became even thinner and more dispersive than that in steel 2 and steel 3. The M/A islands in pipeline steel consisted of the microtwinned martensite plate and retained austenite¹⁴. It can also be seen that there were many subgrains in the matrix phase in steel 1, steel 2 and steel 3.

3.2. Mechanical properties

The mechanical properties of the rolled plates with the above three microstructures are shown in Table 1. The steel 1 with acicular ferrite microstructure showed the tensile strength of 652 MPa, yield strength of 555 MPa, impact toughness of 365 J, indicating the excellent combination of strength and toughness. However, the uniform elongation of 8.3%, yield ratio of 0.85 and *n* value of 0.09 indicating poor deformability. The yield strength, uniform elongation, yield ratio and *n* value of steel 2 and steel 3 which composed mostly of ferrite plus bainite are 457 and 458 MPa, 12.8 and 11.8%, 0.69 and 0.68, and 0.157 and 0.155, respectively, indicating excellent deformability.

Although tensile strength was similar among steel 1, steel 2 and steel 3, their yield strength was obviously

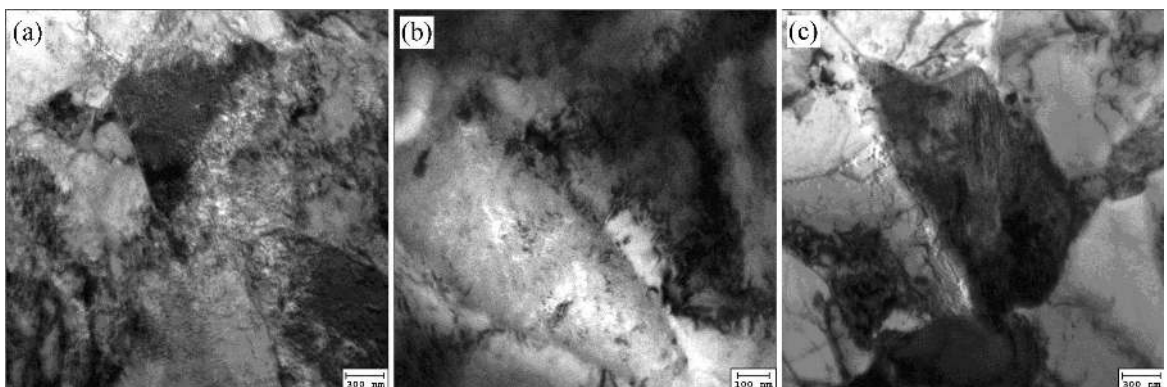


Figure 2. The TEM features of experimental steels (a) steel 1; (b) steel 2; (c) steel 3.

different. Dual-phase microstructure in steel 2 and steel 3 will decrease the yield strength by approximately 100 MPa, thereby leading to the decrease of yield ratio from 0.85 in steel 1 to 0.69 and 0.68 in steel 2 and steel 3. A number of mobile dislocations were formed in ferrite in steel 2 and steel 3, resulting in the decrease of yield strength and the improving of deformability. Acicular ferrite was formed through diffusion and shear transformation mode, so higher-density tangled dislocations were formed in the laths of acicular ferrite, and the effective grain size (EGS) of the AF laths was small. The precipitation of Nb and Ti carbonitrides was remarkable in AF in steel 1, which pinned the dislocations, resulting the improvement of yield ratio. The combined effect of the higher-density tangled dislocations, the small EGS and the remarkable precipitation of Nb and Ti carbonitrides produced the highest yield strength for steel 1^{3,15}.

Although impact toughness in steel 2 and steel 3 was lower than that in steel 1 with AF microstructure, they still satisfied the API-X70 grade steel specification. A little bit

higher impact toughness in steel 1 was due to the much smaller EGS of AF than that of PF in Steel 2 and steel 3^{16,17}. It can also be seen from Table 1 that the mechanical properties of steel 2 and steel 3 were almost the same despite of different microstructure morphology.

The flow behavior of steels can be described by Hollomon Equation (1).

$$\sigma_t = k \varepsilon_t^n \quad (1)$$

Where 'k' is the strength coefficient and 'n' is called the strain hardening exponent. 'n' can indicate the work hardening ability of the material. The higher n value indicates the higher work hardening rate, and the material is preferred for deformation. In this study, n value was 0.09 in steel 1, much lower than those in steel 2 of 0.157 and steel 3 of 0.155.

Figure 3 shows the stress-strain curves of steels investigated. As can be seen from Figure 3, the stress-strain curves of steel 2 and steel 3 exhibited continuous yielding behavior and high hardening rate at early stages of plastic

Table 1. Mechanical properties of steel 1, steel 2 and steel 3.

	Yield strength $R_{0.5}$ (MPa)		Tensile strength R_m (MPa)		$R_{0.5}/R_m$		Elongation (%)		Uniform elongation (%)	
	^a Ave.	^b Std.	Ave.	Std.	Ave.	Std.	Ave.	Std.	Ave.	Std.
Steel 1	555	11.4	652	3.6	0.85	0.010	37	1.5	8.3	0.12
Steel 2	457	11.0	666	1.7	0.69	0.021	45	2.5	12.7	0.10
Steel 3	458	6.2	669	2.6	0.68	0.015	43	2.0	11.8	0.15
	^c Impact toughness A_{kv} (J)		Impact shear area (%)		^d DWTT (%)		n value		k value	
	Ave.	Std.	Ave.	Std.	Ave.	Std.	Ave.	Std.	Ave.	Std.
Steel 1	365	18.0	100	0	96	1.2	0.090	0.005	903.3	7.1
Steel 2	306	27.8	100	0	92	0.8	0.157	0.004	1065.3	13.1
Steel 3	291	29.5	99	0	93	0.9	0.155	0.005	1072.8	24.8

^aAve. denotes average. ^bStd. denotes standard deviation. ^cThe impact and DWTT tests were conducted at 253 K (−20 °C) and 258 K (−15 °C), respectively.

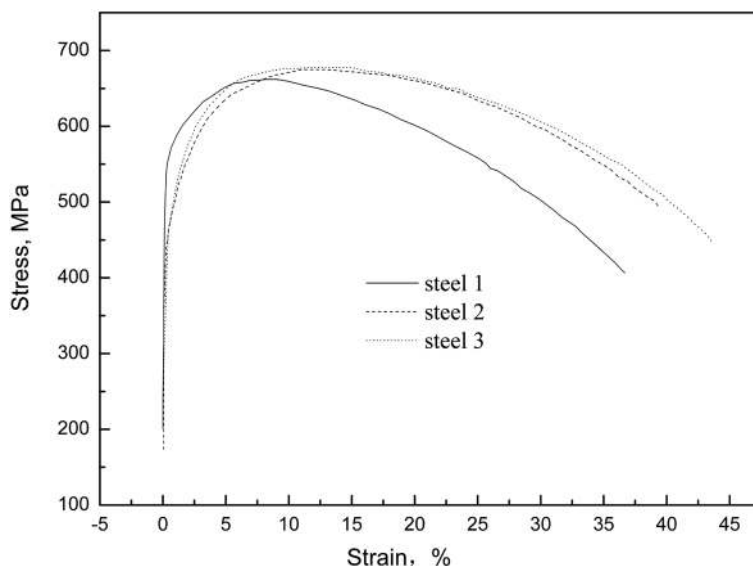


Figure 3. Stress-strain curves of experimental steel.

deformation, which was attributed to a number of mobile dislocations generated by transformation from austenite to bainite phases during cooling process^{18,19}.

As mentioned above, steel 2 and steel 3 possessed lower yield ratio, higher uniform elongation and n value than steel 1, so they exhibited better deformability than steel 1. These variations of properties were related to the microstructural change.

4. Conclusions

The experimental results of this investigation indicate that it is possible to fabricate the ferrite-bainite dual-phase pipeline steel with favorable deformability by suitable TMCP process or intercritical annealing.

(1) Steel 1 by TMCP showed the acicular ferrite microstructure. By adjusting the parameters of TMCP, a dual-phase microstructure of polygonal ferrite plus bainite colonies at ferrite grain boundaries could be obtained in steel

2. By intercritical annealing with steel 1, polygonal ferrite, massive ferrite plus bainite could be obtained in steel 3.

(2) The steel 1 with an acicular ferritic microstructure which was fabricated by TMCP exhibited an excellent combination of strength and toughness, but provided high yield ratio of 0.85, low uniform elongation of 8.3% as well as low strain hardening exponent of 0.09, indicating poor deformability.

(3) In contrast to above steel 1, the steel 2 and steel 3 having a ferrite-bainite dual-phase microstructure respectively fabricated by TMCP and intercritical annealing exhibited the improved deformability in terms of the low yield ratio of 0.69 and 0.68, high uniform elongation of 12.8% and 11.8%, and strain hardening exponent of 0.157 and 0.155. Steel 2 and steel 3 showed satisfied properties such as low yield ratio, high uniform elongation and strain hardening coefficient, and readily satisfied the deformability requirements for X70 steel.

References

- Xiao FR, Liao B, Ren DL, Shan YY and Yang K. Acicular ferritic microstructure of a low-carbon Mn–Mo–Nb microalloyed pipeline steel. *Materials Characterization*. 2005; 54(4-5):305-314. <http://dx.doi.org/10.1016/j.matchar.2004.12.011>.
- Zhao MC, Yang K, Xiao FR and Shan YY. Continuous cooling transformation of undeformed and deformed low carbon pipeline steels. *Materials Science and Engineering A*. 2003; 355(1-2):126-136. [http://dx.doi.org/10.1016/S0921-5093\(03\)00074-1](http://dx.doi.org/10.1016/S0921-5093(03)00074-1).
- Zhao MC, Yang K and Shan YY. Comparison on strength and toughness behaviors of microalloyed pipeline steels with acicular ferrite and ultrafine ferrite. *Materials Letters*. 2003; 57(9-10):1496-1500. [http://dx.doi.org/10.1016/S0167-577X\(02\)01013-3](http://dx.doi.org/10.1016/S0167-577X(02)01013-3).
- Ko YG, Lee CW, Namgung S and Shin DH. Strain hardening behavior of nanostructured dual-phase steel processed by severe plastic deformation. *Journal of Alloys and Compounds*. 2010; 504:S452-S455. <http://dx.doi.org/10.1016/j.jallcom.2010.02.109>.
- Lis J, Lis AK and Kolan C. Processing and properties of C–Mn steel with dual-phase microstructure. *Journal of Materials Processing Technology*. 2005; 162-163:350-354. <http://dx.doi.org/10.1016/j.jmatprotec.2005.02.105>.
- Qu JB, Dabboussi W, Hassani F, Nemes J and Yue S. Effect of microstructure on the dynamic deformation behavior of dual phase steel. *Materials Science and Engineering A*. 2008; 479(1-2):93-104. <http://dx.doi.org/10.1016/j.msea.2007.06.020>.
- Meng QG, Li J, Wang J, Zhang ZG and Zhang LX. Effect of water quenching process on microstructure and tensile properties of low alloy cold rolled dual-phase steel. *Materials & Design*. 2009; 30(7):2379-2385. <http://dx.doi.org/10.1016/j.matdes.2008.10.026>.
- Niakan H and Najafzadeh A. Effect of niobium and rolling parameters on the mechanical properties and microstructure of dual phase steels. *Materials Science and Engineering A*. 2010; 527(21-22):5410-5414. <http://dx.doi.org/10.1016/j.msea.2010.05.078>.
- Bhagavathi LR, Chaudhari GP and Nath SK. Mechanical and corrosion behavior of plain low carbon dual-phase steels. *Materials & Design*. 2011; 32(1):433-440. <http://dx.doi.org/10.1016/j.matdes.2010.06.025>.
- He R and Jin H. Permafrost and cold-region environmental problems of the oil product pipeline from Golmud to Lhasa on the Qinghai–Tibet Plateau and their mitigation. *Cold Regions Science and Technology*. 2010; 64(3):279-288. <http://dx.doi.org/10.1016/j.coldregions.2010.01.003>.
- Tang ZH and Stumpf W. The role of molybdenum additions and prior deformation on acicular ferrite formation in microalloyed Nb–Ti low-carbon line-pipe steels. *Materials Characterization*. 2008; 59(6):717-728. <http://dx.doi.org/10.1016/j.matchar.2007.06.001>.
- Petrov R, Kestens L and Houbaert Y. Characterization of the microstructure and transformation behaviour of strained and nonstrained austenite in Nb–V-alloyed C–Mn steel. *Materials Characterization*. 2004; 53(1):51-61. <http://dx.doi.org/10.1016/j.matchar.2004.07.005>.
- Reip CP, Shanmugam S and Misra RDK. High strength microalloyed CMn(V–Nb–Ti) and CMn(V–Nb) pipeline steels processed through CSP thin-slab technology: Microstructure, precipitation and mechanical properties. *Materials Science and Engineering A*. 2006; 424(1-2):307-317. <http://dx.doi.org/10.1016/j.msea.2006.03.026>.
- Wang CM, Wu XF, Liu J and Xu NA. Transmission electron microscopy of martensite/austenite islands in pipeline steel X70. *Materials Science and Engineering A*. 2006; 438-440:267-271. <http://dx.doi.org/10.1016/j.msea.2006.02.118>.
- Yakubtsov IA, Poruks P and Boyd JD. Microstructure and mechanical properties of bainitic low carbon high strength plate steels. *Materials Science and Engineering A*. 2008; 480(1-2):109-116. <http://dx.doi.org/10.1016/j.msea.2007.06.069>.
- Wang W, Shan YY and Yang K. Study of high strength pipeline steels with different microstructures. *Materials Science and Engineering A*. 2009; 502(1-2):38-44. <http://dx.doi.org/10.1016/j.msea.2008.10.042>.
- Shin SY, Hwang B, Lee S, Kim NJ and Ahn SS. Correlation of microstructure and charpy impact properties in API X70 and X80 line-pipe steels. *Materials Science and Engineering A*. 2007; 458(1-2):281-289. <http://dx.doi.org/10.1016/j.msea.2006.12.097>.

18. Movahed P, Kolahgar S, Marashi SPH, Pouranvari M and Parvin N. The effect of intercritical heat treatment temperature on the tensile properties and work hardening behavior of ferrite–martensite dual phase steel sheets. *Materials Science and Engineering A*. 2009; 518(1-2):1-6. <http://dx.doi.org/10.1016/j.msea.2009.05.046>.
19. Hwang B and Lee CG. Influence of thermomechanical processing and heat treatments on tensile and Charpy impact properties of B and Cu bearing high-strength low-alloy steels. *Materials Science and Engineering A*. 2010; 527(16-17):4341-4346. <http://dx.doi.org/10.1016/j.msea.2010.03.106>.